Magnetic-field effect in organic photoconductive devices studied by time-of-flight

F. Wang, J. Rybicki, K. A. Hutchinson, and M. Wohlgenannt

Phys. Rev. B **83**, 241202 — Published 20 June 2011

DOI: 10.1103/PhysRevB.83.241202

Magnetic-field effect in organic photoconductive devices studied by time-of-flight

F. Wang[1], J. Rybicki[1], K. A. Hutchinson[2], and M. Wohlgenannt[1*]
[1] *Department of Physics and Astronomy, Optical Science and Technology Center, University of Iowa, Iowa City, IA-52242 and*
[2] *Department of Electrical and Computer Engineering, University of Iowa, Iowa City, IA-52242*
(Dated: June 2, 2011)

It is well-established that weak applied magnetic fields of several tens of mT can lead to a change of several percent in the continuous wave photocurrent in organic semiconductor devices. However, it remains to be determined whether the applied magnetic field modifies the photocarrier generation efficiency or their mobility, or both. We use magnetic-field-dependent time-of-flight spectroscopy to disentangle these two possibilities. We find evidence that the magnetic field leads to a decrease in the photocarrier time-of-flight.

Measurable effects due to small magnetic fields (tens of mT) were initially observed in (bio)chemical processes (Ref.[1] and refs. therein). An important example of a system that was studied is the primary reaction in photosynthesis[2]. A technologically important system involving photoexcitations is photoconductivity in organic semiconductor devices, which shows promise for solar energy production. Several studies of the steady-state photocurrent have revealed that it increases by several percent in an applied field of several tens of mT[3–5]. The following mechanism is usually employed to explain this observation: photoexcitation leads to the formation of an initially pure singlet radical pair (a.k.a. polaron pair), but triplet character develops due to hyperfine coupling. Assuming that the back-transfer reaction is different for singlet and triplet pairs, the charge separation efficiency will be affected by applied magnetic fields comparable to the hyperfine coupling strength[3,4]. Consequently, the number of free photocarriers becomes a function of the applied magnetic field.

Recent studies of the organic magnetoresistive effect (Ref.[6] and refs. therein) have revealed a new facet of magnetic field effects: the conductivity in organic semiconductor thin film devices, such as those used for organic light-emitting diodes (OLEDs), is also influenced by small applied magnetic fields. Possible explanations for the organic magnetoresistive effect are more subtle than those for photoconductivity, since any intermediate pair states that may form during the conduction process are formed in a spin-independent manner. Indeed, the mechanism that causes this effect is presently strongly debated. Amongst the models proposed are the bipolaron model[7] and the polaron-triplet scattering mechanism[8] that lead to a magnetic field dependent mobility. Other models where the mobility is field-independent have also been proposed[9–11]. The possibility of a magnetic field effect on the mobility raises an interesting question: is the measured magnetic field effect on the steady-state photocurrent due to a change in carrier generation efficiency, or is it rather caused by a magnetic field effect on the carrier mobility? The proof of a magnetic-field dependent mobility would be of significant importance to the wider field of magnetoresistance, since textbook examples of magnetoresistive devices rely on spin-injection, very large applied magnetic fields, or very low temperature. Organic magnetoresistance does not rely on any of these properties and therefore significantly extends known magnetoresistive mechanisms. Since the carrier time-of-flight is inversely proportional to the mobility, we can test for a magnetic-field dependent mobility by measuring the time-of-flight with and without magnetic field. We performed such experiments on an organic photoconductive device based on a representative organic semiconductor, specifically poly[2-methoxy-5-(2-ethylhexyloxy)-1,4-phenylene-vinylene] (MEH-PPV, see Fig. 1, inset).

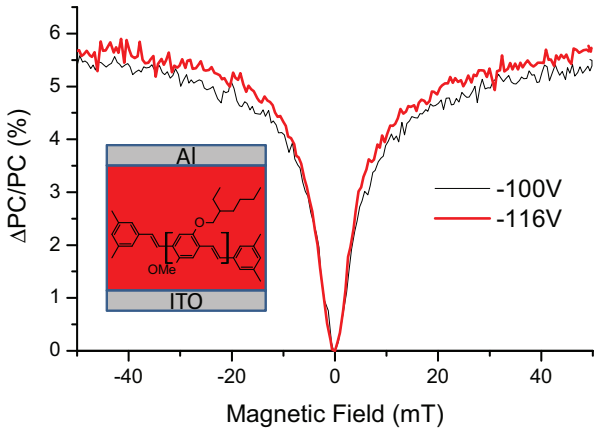

FIG. 1. Magnetic field effect on the continuous wave photocurrent vs. magnetic field for two different reverse biases. Inset: schematic device structure.

Surveying prior work, we note that a recent study of MEH-PPV solar cells[12] using electron-spin-resonance spectroscopy found evidence for bipolaron formation and magnetic field dependent mobility, whereas another study using time-resolved electroluminescence in organic light-emitting diodes could not detect any effect of the magnetic field on the carrier mobility[13]. Using the dark-injection technique Song et al.[14] recently found evidence for field-dependent mobility in devices based on a common small molecule, but only in the bipolar regime.

Our devices were fabricated on indium-tin-oxide (ITO) covered glass slides. The MEH-PPV polymer (American Dye Sources, used as received) film was deposited by drop casting from a 10 mg/ml toluene solution by slow evaporated in a solvent-rich environment resulting

in a 2.9 μm thick film. The residual solvent was removed by baking inside a glove box for 2 hours at 80 ^oC. Finally a semi-transparent, 20 nm thick Al top electrode was deposited by thermal evaporation in high vacuum. The devices were operated in dynamic vacuum at room-temperature. In the devices used for the measurements reported in Fig. 4 the MEH-PPV thickness was 1.5 μm and a charge-generation layer[15] of 50 nm of C_{60} was deposited by thermal evaporation prior to the deposition of the Al layer.

The photocarrier time-of-flight traces were measured as follows: A ThermoLaserScience 337-i model nitrogen pulsed laser was used for pumping a Lasertechnik Berlin UDL 100 dye laser. The output (475 nm, 7ns, 40 μJ/pulse) was focused onto the 0.5x1 mm^2 device area through the semi-transparent Al electrode. The time-resolved photocurrent was sensed using a 1kOhm resistor and recorded on a LeCroy LT 372 digital oscilloscope. We used the oscilloscope-internal averaging function to improve signal-to-noise. We employed a modulation type technique for the magnetic-field dependent time-of-flight measurements. A repeating series of traces was recorded with magnetic field on, off, off, on. This sequence, rather than the simpler on, off sequence was chosen to minimize the effect of temporal sample drift. The fractional change in time-resolved photocurrent was averaged over approximately 50 sequences to achieve a satisfactory signal-to-noise ratio. For comparison, we also measured the magnetic field effect on the continuous wave photocurrent in the same device (Fig. 1). For this measurement, we used an Ar^+ ion laser at 476.5 nm, adjusting the power until the magnitude of the steady state photocurrent equals $\approx 1\mu$A, a value typical for the photocurrent time-of-flight experiment.

The time-of-flight experiment involves photogeneration of a packet of charge carriers (initially confined to within the light absorption length of $\approx$ 100 nm) by illumination with the laser pulse. The drift of the carriers under an external bias to the collecting electrode results in the time-dependent photocurrent. The transit time τ of the carriers is related to the carrier mobility μ via the relation $\mu = d/\tau E$, where d is the film thickness and E the external bias field. We used reverse bias and this corresponds to drift of the holes, which are the species with larger mobility in MEH-PPV. Fig. 2 shows the time-resolved photocurrent (photocarrier time-of-flight experiment) for two different reverse biases. The data exhibit a sharp spike close to zero time, which is related to the experiment's resistance-capacitance (RC) time-constant and determines the time-resolution of the experiment. At longer times the photocurrent decay is visible. The most important feature of the time-of-flight data is the shoulder that is visible in the data around 100 μs, which defines the characteristic carrier time-of-flight. The data at short time decay exponentially, and we extract a RC time-constant of 5 μs. Following common practice we replot the data on log-log scales in the bottom inset. The data was corrected for the RC-related initial spike. The

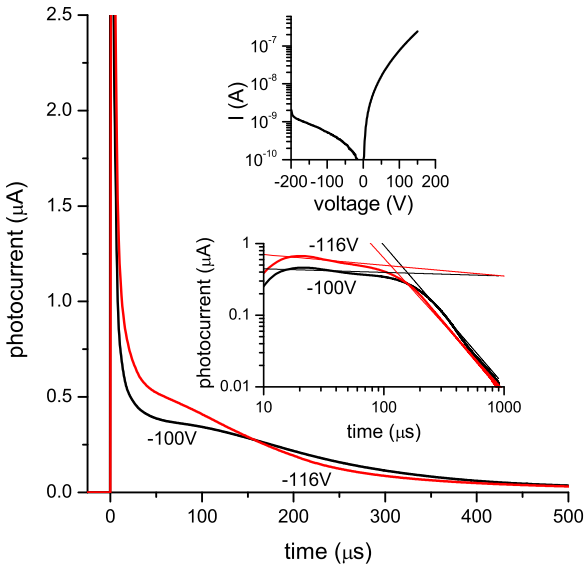

FIG. 2. Time-resolved photocurrent for two different reverse biases. Bottom inset: Same data corrected for the RC-related initial spike on log-log scales. Top inset: Dark current vs. voltage.

log-log plot reveals a clear shoulder that separates data with a small exponent at small times, and a larger exponent at larger times. Such behavior is typical of time-of-flight traces in dispersive materials.

Several theories[16–18] have been developed to account for this observation. An early model was developed by Scher and Montroll[16]. This model does not provide a quantitatively accurate description of dispersive transport in polymer films. However, it is sufficient for our purposes, since we are mainly interested in explaining the effect of a small perturbation on the transit time, and not in obtaining a quantitative model for the transit time itself. We will use this model to analyze the magnetic-field dependent time-of-flight traces to be discussed below. The reader is referred to Refs.[17,18] for more accurate models. A central feature of the Scher-Montroll model is that the waiting time distribution obeys a power law. Bässler[18] pointed out that the power law waiting time distribution is realized in materials such as amorphous inorganic semiconductors where multiple trapping occurs in an exponential trap distribution, but not in organic and polymeric materials, where the hopping site distribution can be well approximated by a Gaussian.

The Scher-Montroll model states that the shoulder occurs at the typical carrier transit time, τ, and gives the following relation for the photocurrent time-dependence:

$$PC = \frac{\alpha Q}{2\tau}\left[\left(\frac{t}{\tau}\right)^{-1+\alpha}, \left(\frac{t}{\tau}\right)^{-1-\alpha}\right] \; for\; t<\tau, t>\tau \quad (1)$$

where $0 < \alpha < 1$ is a parameter that quantifies how dispersive the transport is, and Q is the total charge, i.e.

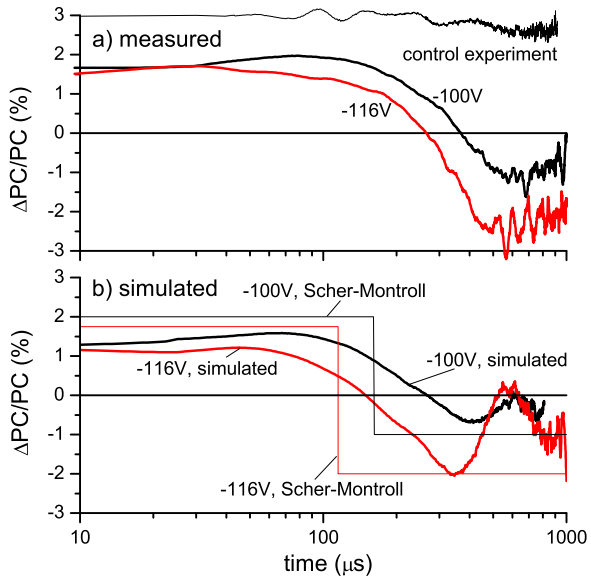

FIG. 3. Magnetic field effect on the time-resolved photocurrent (time-of-flight experiment). a) Measured traces for two different reverse biases and trace for a control experiment (see text). b) Bold lines: Simulated traces for the same two reverse biases (see text). Thin lines: Prediction of Scher-Montroll theory.

the time-integral over the photocurrent. The thin lines in Fig. 2, bottom inset, are fits to the Scher-Montroll expression, yielding $\tau = 161\mu s$, $\alpha = 0.95$ and $\tau = 115\mu s$, $\alpha = 0.85$ for -100 V and -116 V bias, respectively.

The main goal of this work is to examine the effect of an applied magnetic field on the photocarrier time-of-flight traces. Fig. 3 a) shows the measured magnetic field effect on the time-resolved photocurrent (time-of-flight experiment) for two different reverse biases. The data give the fractional change $\Delta PC/PC = (PC(100mT) - PC(0))/PC(0)$ in the time-resolved photocurrent. The figure shows that $PC(100mT)$ is initially 2% and 1.5% larger than $PC(0)$ for -100 V and -116 V bias, respectively, but for larger times it drops below $PC(0)$.

The results shown in Fig. 3 are inconsistent with the scenario that the applied B-field simply increases the number of photogenerated carriers[3,4]. In this simple model, the photogenerated polaron pairs are initially bound by the Coulomb interaction and thus do not contribute to the photoconductivity. These pairs are produced from a singlet exciton precursor and are therefore initially in a pure singlet state. However, their spin evolves under hyperfine interaction, and all four spin states of the pair (one singlet and three triplets) become populated. An external magnetic field large compared to the hyperfine coupling, however, lifts the degeneracy of the triplet states, and thus prevents mixing between the singlet and two of the three triplet substates. The pairs will either recombine geminately to form singlet or triplet excitons or dissociate into free charge carriers that result in photocurrent. If the geminate recombination rate for the singlet channel and the triplet channel is different, an applied magnetic field will therefore shift the number of photocarriers produced.

The processes we have described so far occur on a nanosecond time-scale[1]. Compared to the time-scales relevant to our time-of-flight experiment (100 μs) this corresponds to an instantaneous change in the photocarrier generation efficiency and should therefore result in a flat, i.e. time-independent fractional enhancement of the photocurrent. To confirm this expectation, we performed the following control experiment: We periodically inserted a glass slide into the laser path in order to modulate its intensity. During the times without the glass slide in the laser path additional carriers are generated, simulating the action of the magnetic field that enhances photocarrier generation. Fig. 3 shows that the resulting traces are indeed flat, i.e. time-independent.

The time-dependent $\Delta PC/PC$ traces we observe (see Fig. 3) can only be understood when analyzed using the scenario that the photocarriers also experience an enhanced mobility in the applied magnetic field. As a result of the enhanced mobility, the photocarrier transit times will be reduced and the photocurrent will consequently decay faster, resulting in a smaller current at large times, and correspondingly, larger current at smaller times. Assuming a constant total charge Q, the Scher-Montroll formula predicts a fractional increase (decrease) in photocurrent equal to $-\alpha\Delta\tau/\tau$ for times less than (greater than) τ, in qualitative agreement with our experimental observations. Because the experimental data do not show a strictly equal enhancement (decrease) in photocurrent at times less than (greater than) τ, we also allow an overall change in charge carrier generation efficiency, i.e. Q, which leads to a time-independent shift in $\Delta PC/PC$. Fig. 3 b) thin lines shows the prediction of the Scher-Montroll formula. The best agreement between theory and experiment is achieved for the following parameters: 1.6% (2.2%) decrease in τ and 0.5% (-0.25%) increase in Q for -100V (-116V) bias.

The abrupt change from positive to negative magnetic field effect at τ cannot, of course, be taken seriously, and in reality a rounded transition is expected. To illustrate this, we perform a second analysis analogous to that based on Scher-Montroll theory, but this time using the experimental time-of-flight traces for zero field (Fig. 2) for the simulation. We simulate the action of the magnetic field by the following mathematical manipulations. We shrink the time scale of the zero-field data by a constant to simulate the change in τ, and also multiply the photocurrent scale by the same constant to simulate the increased mobility that corresponds to a smaller transit time. This yields the expected high-field data. We then calculate the fractional change $\Delta PC/PC$ between simulated high-field data and the zero-field data. Again, we actually performed a more general analysis also allowing a change in photocarrier generation efficiency (Q). The best agreement between simulation (Fig. 3 b) and actual data (Fig. 3 a) is achieved with a 1.4% (1.4%) decrease

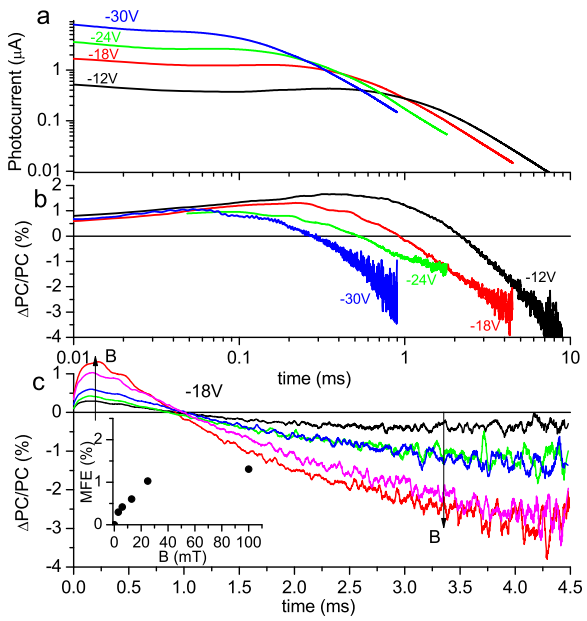

FIG. 4. a) Time-of-flight traces at different bias voltages in an ITO/MEH-PPV/C_{60}/Al device. b) Magnetic field effect, $\Delta PC/PC$, on the time-resolved photocurrent for the same bias voltages. c) Magnetic field effect on the time-resolved photocurrent at -18V bias for different applied magnetic fields, B = 3, 6, 13, 25, 100 mT. Inset: Dependence of $\Delta PC/PC$ at 250 μs on B.

in τ and 0.4% (0.15%) increase in Q for -100V (-116V) bias.

Fig. 4 a) shows the dependence of the TOF traces on the bias voltage in ITO/MEH-PPV/C_{60}/Al devices. The C_{60} layer was inserted to promote photocarrier generation at the MEH-PPV/C_{60} interface[15]. This significantly improves signal to noise and also allows us to measure at lower bias voltage and correspondingly larger transit time. As expected, the transit time decreases with increasing bias. Fig. 4 b) shows that the cross-over point between positive and negative ΔPC correspondingly shifts to smaller τ. Next we confirm that the B-dependence of the TOF traces is indeed related to the hyperfine mechanism. For this purpose we report $\Delta PC/PC$ for several different applied B in Fig. 4 c). The inset shows $\Delta PC/PC$ at 250 μs vs. B. The resulting dependence is very similar to that of the steady-state effect (Fig. 1), and agrees with those commonly reported for magnetic-field effects cause by the hyperfine mechanism[3,4].

In summary, we showed that small magnetic fields can lead to a change in the photocarrier time-of-flight. This change reflects a change in mobility. Two mechanisms for a mobility sensitive to small magnetic fields have recently been proposed, the bipolaron[7] model and the triplet-polaron scattering mechanism[8]. Which of these mechanisms is responsible for the observed magnetic-field-dependent mobility? For a careful interpretation of the data, the polymer film thickness must be divided into two regions, the excitation region which extends over the first $\approx$ 100 nm, and the purely unipolar transport region which extends over the remaining $\approx$ 95% of the film. Scattering with triplets could occur only in the excitation region (strictly speaking triplets may diffuse out of this region, but the room-temperature diffusion length for triplets in polymer films is only $\approx$ 100 nm[19]). Our results are therefore consistent with the bipolaron mechanism, although a small contribution of the polaron-triplet mechanism is possible. We note that a recent work[14] detected a magnetic-field induced change in mobility in bipolar OLEDs, which they assigned to the action of the polaron-triplet mechanism. It is important to prevent a significant injection of minority carriers at the counter electrode, since these minority carriers could recombine with the arriving package of majority carriers, leading to additional photocurrent decay at long times. Fig. 2 top left inset shows the dark current measurement. At the reverse biases employed, the dark current is two orders of magnitude less than the photocurrent, excluding a significant contamination from recombination of the long-time time-of-flight traces. Low minority carrier injection was to be expected, since the workfunction of the ITO electrode is unsuitable for electron injection. Finally, we note that the magnetic field effect on the continuous-wave photocurrent (Fig. 1) is 2-3 times larger than that in the time-of-flight data (Fig. 3). A possible explanation for this observation within the bipolaron model is that the larger steady state carrier concentration in the cw experiment leads to more frequent polaron-polaron encounters.

This work was supported by Army MURI Grant No. W911NF-08-1-0317 and NSF Grant No. ECS 07-25280.

* markus-wohlgenannt@uiowa.edu

[1] K. Schulten, Fertkorperprobleme-Adv. Solid State Phys. **22**, 61 (1982).
[2] A. J. Hoff, Q. Rev. Biophys. **14**, 599 (1981).
[3] E. L. Frankevich et al., Phys. Rev. B **46**, 9320 (1992).
[4] J. Kalinowski, J. D. Szmytkowski, and W. Stampor, Chem. Phys. Lett. **378**, 380 (2003).
[5] P. Desai, P. Shakya, T. Kreouzis, and W. P. Gillin, Phys. Rev. B **76**, 235202 (2007).
[6] O. Mermer et al., Phys. Rev. B **72**, 205202 (2005).
[7] P. A. Bobbert et al., Phys. Rev. Lett. **99**, 216801 (2007).
[8] P. Desai et al., Phys. Rev. B **75**, 094423 (2007).
[9] V. N. Prigodin, J. D. Bergeson, D. M. Lincoln, and A. J. Epstein, Synthetic Metals **156**, 757 (2006).
[10] B. Hu and Y. Wu, Nat. Mater. **6**, 985 (2007).
[11] F. J. Wang, H. Bassler, and Z. V. Vardeny, Phys. Rev. Lett. **101**, 236805 (2008).
[12] J. Behrends et al., Phys. Rev. Lett. **105**, 176601 (2010).
[13] F. Li, L. Y. Xin, S. Y. Liu, and B. Hu, Appl. Phys. Lett. **97**, 073301 (2010).
[14] J. Y. Song et al., Phys. Rev. B **82**, 085205 (2010).
[15] M. Xu, W. B. Huang and J. B. Peng, Chinese Sci. Bull. **55**, 1859 (2010).
[16] H. Scher and E. W. Montroll, Phys. Rev. B **12**, 2455 (1975).
[17] M. Van der Auweraer, F. C. De Schryver, P. M. Borsenberger and H. Bassler, Adv. Mater. **6**, 199 (1994).
[18] H. Bassler, Phys. Stat. Sol. (b) **175**, 15 (1993).
[19] A. Kohler and H. Bassler, Mater. Sci. Eng. R-Rep. **66**, 71 (2009)
.